

Stationary Properties of a Randomly Driven Ising Ferromagnet

Johannes Hausmann[†] and Pál Ruján^{†,§}

Fachbereich 8 Physik[†] and ICBM[§], Postfach 2503, Carl von Ossietzky Universität, D-26111 Oldenburg, Germany
(September 11, 2018)

We consider the behavior of an Ising ferromagnet obeying the Glauber dynamics under the influence of a fast switching, random external field. Analytic results for the stationary state are presented in mean-field approximation, exhibiting a novel type of first order phase transition related to dynamic freezing. Monte Carlo simulations performed on a quadratic lattice indicate that many features of the mean field theory may survive the presence of fluctuations.

05.50+g 05.70.Jk 64.60Cn 68.35.Rh 75.10.H 82.20.M

Many information processing systems, natural or artificial, have a macroscopic number of connected elements subject to external stimuli changing faster than the characteristic thermal relaxation time. However, attempts at handling nonequilibrium stationary states of such systems have been made only recently [1]. As illustrated by the randomly driven Ising model presented in this Letter, stationary states far from equilibrium might be many times more effective in dynamically storing information than thermal equilibrium states.

The Ising ferromagnet in a time-dependent sinusoidally oscillating field has received recently a lot of attention, from both a theoretical and experimental point of view. On the theoretical side, Rao, Krishnamurthy, and Pandit [2] have presented a large N -expansion of the cubic $O(N)$ model in three dimensions and calculated the critical exponents related to the area of the hysteresis loop. The underlying dynamic phase transition has been then studied within both mean-field [3] and Monte Carlo simulations [4–7]. The theory presented in this paper is a generalization of these ideas for the case when the external field is generated by chaotic dynamics and/or is a random variable.

Let a spin system $\vec{\mu} = (s_1, s_2, \dots, s_i, \dots, s_N)$, $s_i = \pm 1$, be in *local* thermal equilibrium and denote by $P(\vec{\mu}, t)$ the probability of finding the system in state $\vec{\mu}$ at time t . The Master Equation used first by Glauber [8] for defining a stochastic dynamics for the Ising model reads then

$$\frac{dP(\vec{\mu}; t)}{dt} = \sum_i^N w(\vec{\mu}|\vec{\mu}_i)P(\vec{\mu}_i; t) - P(\vec{\mu}; t) \sum_i^N w(\vec{\mu}_i|\vec{\mu}) \quad (1)$$

where $\vec{\mu}_i = (s_1, s_2, \dots, -s_i, \dots, s_N)$. $w(\vec{\nu}|\vec{\mu})$ denotes the transition rate from configuration $\vec{\mu}$ into state $\vec{\nu}$. Note that $P(\vec{\mu}; t)$ can be represented as a 2^N dimensional vector. It is useful to expand $P(\vec{\mu}, t)$ in the orthonormal basis formed by all possible spin products, $P(\vec{\mu}; t) = \frac{1}{2^N} \sum_{\alpha} \pi_{\alpha} \prod_{i \in \alpha} s_i$, where $\pi_{\alpha} = \langle \prod_{i \in \alpha} s_i \rangle_t$ [8]. In this ‘spin-correlation basis’ the time-dependent distribution is given by $\vec{\pi}(t)$. The spectrum of the Liouville operator $\hat{\mathcal{L}}$

$$\frac{d\vec{\pi}}{dt} = -\hat{\mathcal{L}}_{B(t)}\vec{\pi}(t) \quad (2)$$

is invariant under such orthogonal transformations. The slowest relaxation time corresponds to the decay of the order parameter (the total magnetization) and is denoted by τ_{sys} . The typical phonon-spin interaction time is $\tau_{spin-flip} \ll \tau_{sys}$. In what follows we assume that the external field B is a random variable sampled identically and independently at discrete times $t_n = n\tau_B$, ($n = 0, 1, \dots$) from the symmetric distribution:

$$\rho(B(t_n)) = \frac{1}{2}\delta(B(t_n) - B_0) + \frac{1}{2}\delta(B(t_n) + B_0) \quad (3)$$

As long as $\tau_B \gg \tau_{sys}$ the spin system relaxes to global thermal equilibrium. The situation is very different if $\tau_{sys} \gg \tau_B \gg \tau_{spin-flip}$. Now the stationary state is determined by the distribution of the external field. By integrating Eq. (1) over the $(t_n, t_n + \tau_B)$ intervals, one obtains a ‘coarse grained’ discrete Master Equation

$$\frac{\vec{\pi}(t_n + \tau_B) - \vec{\pi}(t_n)}{\tau_B} = -\hat{\mathcal{L}}_{B(t_n)}\vec{\pi}(t_n) \quad (4)$$

which still describes correctly the long-time behavior of Eq. (1). Eqs. (3-4) map our problem into an iterated function system (IFS) [16].

The invariant probability density $\mathcal{P}_s[\vec{\pi}]$ induced by the dynamics (4) satisfies the Chapman-Kolmogorov equation:

$$\mathcal{P}_s(\vec{\pi}) = \int d\vec{\pi}' \mathcal{P}_s(\vec{\pi}') \int dB \rho(B) \delta(\vec{\pi} - e^{-\hat{L}_B \tau_B} \vec{\pi}') = \left[\delta(\vec{\pi} - e^{-\hat{L}_B \tau_B} \vec{\pi}') \right] \equiv \hat{K} \mathcal{P}_s(\vec{\pi}) \quad (5)$$

where $[A]$ denotes the dynamic average $\int d\vec{\pi}' \mathcal{P}_s(\vec{\pi}') \int dB \rho(B) A$ and \hat{K} the Frobenius-Perron operator.

As an example we consider the mean field Ising model. In this case all multispin correlations factorize in the thermodynamic limit and the stationary distribution depends solely on the total magnetization. The energy is defined as usual,

$$E = -\frac{J}{N} \sum_{i \neq j} s_i s_j - \mu_B B \sum_i s_i \quad (6)$$

where μ_B is the Bohr-magneton. For the transition rate $w(\vec{\mu}_i | \vec{\mu})$ we use the Glauber-form

$$w(\vec{\mu}_i | \vec{\mu}) = \frac{1}{2\alpha} [1 - s_i \tanh(\frac{K}{N} \sum_{j \neq i} s_j + H)] \quad (7)$$

where $\beta = 1/k_B T$, $K = \beta J$, $H = \beta \mu_B B$ and α sets the time constant. Applying Eq. (4) one obtains after performing the thermodynamic limit $N \rightarrow \infty$:

$$m(t+1) = \tanh(Km(t) + H(t)), \quad (8)$$

where time is measured in units of τ_B . The field distribution Eq. (3) leads to the one-dimensional map

$$m(t+1) = \begin{cases} \tanh(Km(t) + H_0) & \text{with prob. } \frac{1}{2} \\ \tanh(Km(t) - H_0) & \text{with prob. } \frac{1}{2} \end{cases} \quad (9)$$

Since in the stationary state, Eq. (5), $[m^k(t+1)] = [m^k(t)]$, using Eq. (8) and simple algebraic manipulations we obtain that the k -th moment of the stationary magnetization is given by

$$[m^k] = \left[\left(\frac{v+h}{1+vh} \right)^k \right] \quad k = 1, 2, \dots \quad (10)$$

where $v = \tanh(Km)$ and $h = \tanh(H)$. For example, when expanding up to fourth order in $h_0 = \tanh(H_0)$ we get for the second moment

$$[m^2] \simeq \frac{h_0^2}{1 - K^2(1 - 4h_0^2 + 3h_0^4)} \quad (11)$$

Higher moments can be calculated recursively in full analogy to methods introduced in [9].

The two graphs below, Figs. 1 and 2, show how the map Eq. (9) changes between high and low temperature. For further use let us denote by m_1 , m_2 , and m_3 the possible fixed points of the equation $m = \tanh(Km + H_0)$ in descending order. The stationary magnetization distribution undergoes a tangential bifurcation at the critical field

$$H_c = \frac{1}{2} \ln \frac{1 - m^\dagger}{1 + m^\dagger} + K m^\dagger \quad (12)$$

where $m_2 = m_3 = m^\dagger = \pm \sqrt{\frac{K-1}{K}}$ for $K > 1$. The corresponding phase diagram is shown in the upper part of Fig. 3. Below the phase transition the stationary magnetization distribution bifurcates into two symmetric, stable ‘spontaneous magnetization distributions’ and a central repeller. The phase transition is first order, the average stationary magnetization jumps at the phase border.

A different kind of transitions are related to the analytic structure of the invariant density. Following the notation introduced in [17], one can identify a singular-continuous density with fractal support (SC-F) in both the paramagnetic and the ferromagnetic phase. When a gap opens between the upper and the lower branch of the map the invariant distribution has a fractal support with the capacity dimension $d_0 < 1$. The border of the (SC-F) region is given by $Km_1 = H_0$ in the para- and $K(m_1 + m_3) = 2H_0$ in the ferromagnetic phase. In the region between $d_0 = 1$ and $d_\infty = 1_-$ the distribution is singular-continuous with Euclidean support (SC-E) [17]. Using the ideas developed in [10], we obtain $d_\infty = 1$ if $K(1 - m_1^2) = \frac{1}{2}$. The density distribution is absolutely continuous (AC) if all generalized

dimensions [15] equal one, $d_q = 1$, ($q = 0, \dots, \infty$). These results are graphically summarized in the lower part of Fig. 3.

The generalized free energy of such a driven system can be defined as $-\beta\mathcal{F} = \Lambda$, where Λ is the largest Lyapunov exponent of the map Eq. (9). As expected, in the thermodynamic limit we obtain a dynamic average over the thermal mean field free energy at magnetization m . After performing the average over $\rho(B)$ the generalized free energy per spin is given by

$$-\frac{\beta\mathcal{F}}{N} = \int dm \mathcal{P}_s(m) \frac{1}{2} \ln 2 (\cosh(2Km) + \cosh(2H_0)) \quad (13)$$

Strictly speaking, Eq. (13) is the average free energy. When considering a finite system or a long but finite dynamic trajectory, the free energy is normally distributed. As shown in [12] for the one dimensional random field Ising model, in the SC-F region the multifractal spectrum can be directly related to the second cumulant of the free energy distribution. The arguments presented in [12] apply also to our case, a broad multifractal distribution leads to large free energy fluctuations.

Consider now Fig. 2 at negative magnetization values. Close to but above the critical field (12) the upper branch of the map comes close but does not touch yet the diagonal. Let n be the average number of iterations needed to pass through this region starting from the lower corner by following the upper branch of the map. According to the general theory of type-I intermittency in one-dimensional maps, $n \sim (H_0 - H_c)^{-1/2}$. Since in each iteration step the probability of jumping back along the lower branch is $1/2$, the total time spent in the lower corner is proportional to 2^n , or

$$\tau \sim 2^n \sim 2^{c[H_0 - H_c]^{-\frac{1}{2}}} \quad (14)$$

with $c \sim O(1)$ a constant. This behavior suggests a *dynamic freezing* transition (for more details see [14]).

In order to test the predictions of the mean field theory in a more realistic setting, we performed Monte Carlo simulations for an Ising model with nearest neighbor interactions on a square lattice. The driving field is sampled from the distribution Eq. (3) after each Monte Carlo step (MCS). The left side of Fig. 4 shows the measured magnetization distribution in the paramagnetic phase, which is similar to Fig. 1. Below the critical temperature one obtains distributions similar to the ones displayed on the right side of Fig. 4, to be compared with Fig. 2. Note that the critical field $H_c(K)$ is not a universal quantity and the square lattice values are different from the mean field ones. More details will be published elsewhere. Thermal fluctuations and finite size effects wash out the fine structure of the multifractal magnetization distribution predicted by the mean-field theory. However, the sharp peaks and the presence of gaps indicate that at least the main features of the magnetization distribution are preserved in two-dimensions.

Besides the theoretical interest in describing such systems, we believe that our predictions can be tested with recently developed experimental techniques. Dynamic magnetization measurements have been recently performed in ultrathin Au(111)/Cu(0001)/Au(111) sandwiches or epitaxial Co/Au(111) films [18–20]. Similarly, hysteresis measurements on the ultrathin film Co/Au(001) [21] indicate that below T_c these systems undergo a dynamic phase transition belonging to the Ising-universality class. More relevant to our theory, the time evolution of magnetization clusters can be optically recorded. The typical relaxation times range from minutes to a few seconds with increasing field amplitudes [20]. This relatively slow relaxation rate allows for a simple experimental realization of the randomly driven external field.

Ultrathin films are potential candidates for magneto-optical storage devices. At well chosen control parameters the stationary magnetization distribution of the RDIM displays several well separated peaks. Hence, by coding appropriately the time-sequence of field switches, one can - *in principle* - store locally more than two binary states.

We are grateful to U. Ramacher and the ZFE, Siemens AG for the SYNAPSE1/N110 neurocomputer, on which the Monte Carlo simulations were performed. This work was partly supported by the DFG through SFB 517.

-
- [1] G. Gallavotti and E. G. D. Cohen, Phys. Rev. Lett. **74** 2694 (1995); J. Stat. Phys. **80** 931 (1995)
 - [2] M. Rao, H. R. Krishnamurthy, and R. Pandit, Phys. Rev. B **42** (1990) 856
 - [3] T. Tomé and M. J. de Oliveira, Phys. Rev. A **41** (1990) 4251

- [4] W. S. Lo and R. A. Pelcovits, *Phys. Rev. A* **42** (1990) 7471
- [5] S. Sengupta, Y. Marathe, and S. Puri, *Phys. Rev. B* **45** (1992) 7828
- [6] P. A. Rikvold, H. Tomita, S. Miyashita, and S. W. Sides, *Phys. Rev. E* **49** (1994) 5080
- [7] S. W. Sides, R. A. Ramos, P. A. Rikvold, and M. A. Novotny, preprint Florida State University, Tallahassee, HD-09 (1996)
- [8] R. J. Glauber, *J. Math. Phys.* **4** 294 (1963)
- [9] G. Györgyi and P. Ruján, *J. Phys. C* **17** 4207 (1984)
- [10] S. N. Evangelou, *J. Phys. C* **20** L511 (1987)
- [11] P. Szépfalusy and U. Behn, *Z. Phys. B* **65** 337 (1987)
- [12] J. Bene and P. Szépfalusy, *Phys. Rev. A* **37** 1703 (1988)
- [13] J. Bene, *Phys. Rev. A* **39** 2090 (1989)
- [14] J. Hausmann and P. Ruján, The randomly driven Ising ferromagnet, submitted for publication
- [15] H. G. E. Henshel and I. Procaccia, *Physica D*, **8** 435 (1983)
- [16] M. F. Barnsley and S. Demko, *Proc. R. Soc. Lond. A* **399** 243 (1985)
- [17] G. Radons, *J. Stat. Phys.* **72** 227 (1993)
- [18] G. Bayreuther, P. Bruno, G. Lugert, and C. Turtur, *Phys. Rev. B* **40** 7399 (1989)
- [19] J. Pommier, P. Meyer, G. Pénissard, J. Ferré, P. Bruno, and D. Renard, *Phys. Rev. Lett.* **65** 2054 (1990)
- [20] R. Allensbach, M. Stampanoni, and A. Bischof, *Phys. Rev. Lett.* **65** 3344 (1990)
- [21] Y.-L. He and G.-C. Wang, *Phys. Rev. Lett.* **70** 2336 (1993)

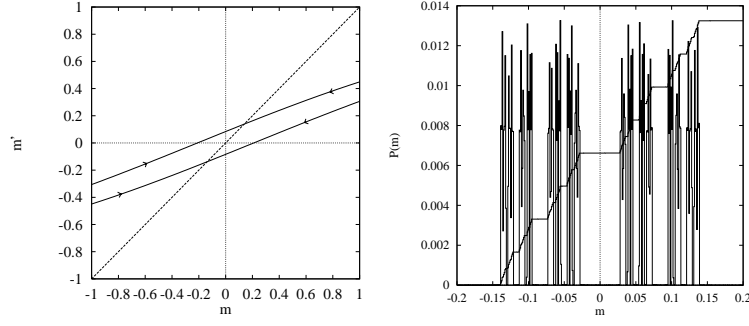


FIG. 1. Mean field map and the stationary distribution in the paramagnetic phase ($K = 0.4$ and $H_0/K = 0.21$).

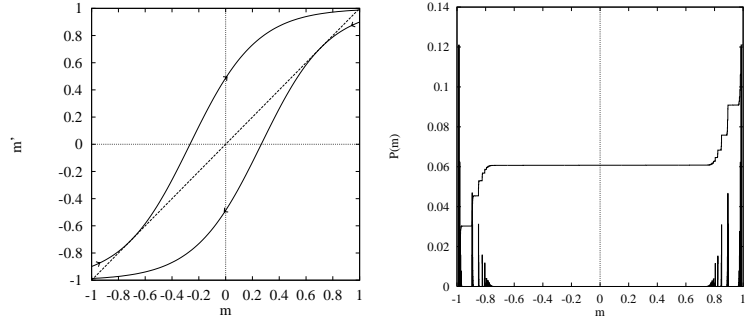


FIG. 2. Same as in Fig. 1 but close to the critical field value ($K = 2.0$ and $H_0/K = 0.266$). Two disjoint distributions are created around the stable fixed points, a repeller in the middle.

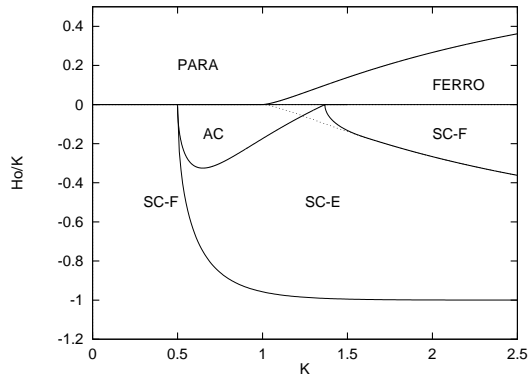


FIG. 3. Mean field phase diagram. The upper part ($H_0 > 0$) shows the border between the para- and ferromagnetic phase. In the lower part ($H_0 < 0$) the regions denoted by SC-F, SC-E correspond to a singular-continuous invariant density with fractal and Euclidean support, respectively, while in the AC-region the density is absolutely-continuous. Note that the diagram is actually symmetric in H_0 .

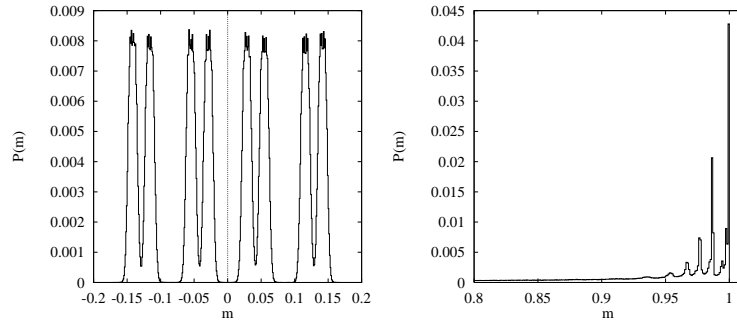


FIG. 4. Left: Magnetization distribution for the square lattice RDIM averaged over eight different initial conditions. $K/K_c = 0.4$, $K_c = 0.4407$, $H_0/K = 0.5$, lattice size 415×415 . The simulation was run for $2 \cdot 10^5$ MCS. Compare to Fig. 1. Right: Same parameters but $K = 2K_c$, $H_0/K = 1$. Compare to Fig. 2.